Heliyon 9 (2023) e19624

Contents lists available at ScienceDirect

Heliyon

journal homepage: www.cell.com/heliyon

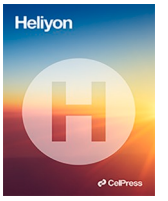

Preparing epoxidized vegetable oil from waste generated by the kapok fiber industry and assessing its thermal stabilization effect as a co-stabilizer for polyvinyl chloride

I Dewa Gede Arsa Putrawan [a,*], Adli Azharuddin [a], Jumrawati Jumrawati [b]

[a] *Chemical Engineering Product Design and Development Research Group, Faculty of Industrial Technology, Institut Teknologi Bandung, Jalan Ganesha 10, Bandung, 40132, Indonesia*

[b] *Master Program in Chemical Engineering, Faculty of Industrial Technology, Institut Teknologi Bandung, Jalan Ganesha 10, Bandung, 40132, Indonesia*

ARTICLE INFO

Keywords:
Co-stabilizer
Epoxidized vegetable oil
Kapok seed oil
Performic acid
Polyvinyl chloride
Thermal stabilizer

ABSTRACT

This paper describes the epoxidation of vegetable oil derived from waste kapok seeds using performic acid, which was generated in situ with sulfuric acid acting as a catalyst. The mole ratio of formic acid to double bonds varied between 0.25 and 1.00. The completion of the reaction has been verified by analyzing FTIR and NMR spectra. The resulting epoxidized kapok seed oil (EKSO) has a maximum oxirane oxygen content of 2.7%, achieved at a formic acid to double bond mole ratio of 0.5. The study has also examined the potential use of EKSO as a co-stabilizer in the presence of Ca/Zn stearate for stabilizing polyvinyl chloride (PVC). Both static and dynamic tests demonstrated that incorporating EKSO into the Ca/Zn stearate system leads to a significant increase in the thermal stability of PVC. Moreover, the effectiveness of EKSO as a co-stabilizer was found to be comparable to that of epoxidized soybean oil (ESBO). However, the use of EKSO did result in a decrease in the strength of PVC due to an increase in plasticity, although this effect was minimal at low dosages and was also observed with ESBO. On the other hand, when utilizing small doses (<2 phr), there is a tendency for flowability to decrease, but the reduction is not significant either. Overall, these findings suggest that EKSO could be a valuable co-stabilizer for PVC in industrial applications, as it enhances PVC's thermal stability without significantly compromising its mechanical and flow properties.

1. Introduction

Kapok fiber is a natural product obtained from the fruits of the silk-cotton or kapok tree (*Ceiba pentandra*) [1]. Kapok is of the *Malvaceae* family and is cultivated and is widely spread in several plantations in Southeast Asia, with most of the countries producing and exporting kapok fiber [2]. Kapok fiber is used for pillows, bedding, soft-toy stuffing, life jackets, and insulation against sound and heat [3]. The global market size of kapok fiber is projected to reach US$ 975.2 million by 2027, growing at a CAGR of 4.2% during 2022–2027 [4]. Kapok fiber production generates kapok seeds as waste, estimated at 1.4–1.7 tons per ton of fiber. These seeds contain 17-20%-w of kapok seed oil (KSO) which is rich in unsaturated fatty acids (53–84%-w) [5]. However, KSO also contains up to 15% cyclopropenoid fatty acids [6], which are toxic, rendering KSO unsuitable for consumption as an edible oil [7–10]. Various non-edible

* Corresponding author.
E-mail address: idewa@itb.ac.id (I.D.G.A. Putrawan).

https://doi.org/10.1016/j.heliyon.2023.e19624
Received 5 April 2023; Received in revised form 18 July 2023; Accepted 28 August 2023
Available online 30 August 2023

applications for KSO have been explored, including biodiesel [11–15], nanofluid [16,17], bio-lubricant [18], and antibacterial [19].

Polyvinyl chloride (PVC) is the most versatile thermoplastic polymer after polyethylene and polypropylene around the world [20]. To prevent thermal degradation due to instability at processing temperatures, a thermal stabilizer is necessary when working with PVC resin [21–24]. Ca/Zn-based thermal stabilizers are commonly utilized in the industry due to their cost-effectiveness and environmental friendliness, as opposed to conventional lead-based thermal stabilizers which are being phased out in many regions [25–27]. Ca/Zn-based thermal stabilizers are typically prepared from fatty materials, such as stearic acid. However, their effectiveness is still mild, so a co-stabilizer (secondary thermal stabilizer) is needed to increase their efficacy [28]. Epoxidized vegetable oil, prepared by epoxidizing the unsaturated part of vegetable oil, is one of the most popular groups of co-stabilizers [29]. The commonly used epoxidized vegetable oil in the PVC industry is epoxidized soybean oil (ESBO) [30]. Other vegetable oils, such as sunflower oil [31–33], rubber seed oil [29,34], and silkworm pupae oil [35] have also been studied in epoxidized forms to stabilize PVC. KSO contains a large amount of unsaturated fraction, making it very promising for use as a raw material for producing epoxy-based co-stabilizers.

Waste utilization is a key element of a circular economy, which aims to accelerate the achievement of sustainable development [36]. The use of KSO as a raw material for producing co-stabilizers is in line with this goal. It not only increases the value of the kapok fiber industry but also provides an alternative raw material for co-stabilizers, without disrupting the supply of edible oil. Despite its potential, KSO has not been explored as a raw material for a co-stabilizer for PVC. The objective of this research is to synthesize epoxidized KSO (EKSO) and evaluate its thermal stabilizing effect on PVC in the presence of a Ca/Zn stearate.

2. Materials and methods

2.1. Materials

Kapok seeds were sourced from a local household scale kapok fiber industry, while formic acid (≥98%), hydrogen peroxide solution (30%), sulfuric acid (≥97%), and n-hexane (≥97%) were purchased from Merck and used without purification. Potassium hydroxide (≥85%), ethanol (≥99.5%), and iso-propanol (≥99.5%) were used for acid value measurement. Additionally, potassium hydroxide and ethanol were utilized for determining saponification value, along with hydrochloric acid solution (37%). For the determination of hydroxyl number, acetic anhydride (≥98%) and pyridine (≥99.0%) were used in conjunction with potassium hydroxide and ethanol. Iodine value measurement involved the use of chloroform (≥99%), Wijs reagent (0.1 mol ICl/liter), potassium iodide (≥99.0%), and sodium thiosulphate (≥98.0%). Oxirane oxygen determination utilized hydrogen bromide in acetic acid solution (33%) and chlorobenzene (≥99.5%). All the chemicals used for analysis were procured from Merck. PVC resin (K value of 65) was provided by Asahimas Chemical Company of Indonesia. All the chemicals used for PVC resin formulation, namely zinc stearate, calcium stearate, stearic acid, paraffin wax, chlorinated polyethylene, polyacrylic (PA-20), and calcium carbonate, were sourced from local suppliers and of industrial grades.

2.2. Oil extraction

The extraction was performed using a Soxhlet apparatus, equipped with a 250 ml capacity extraction chamber and utilizing n-hexane as the solvent. Initially, the kapok seeds were crushed until they could pass through a 10 mesh sieve. Subsequently, the crushed seeds were placed in a filter paper thimble. The thimble was then inserted into the Soxhlet extraction chamber, which was connected to a 1000 ml round bottom flask containing a predetermined amount of solvent. The flask was heated using a heating mantle to facilitate solvent evaporation, with the evaporated solvent condensing through a condenser mounted on the top of the extraction chamber. Tap water was employed as the cooling medium. The condensed solvent effectively wetted the seeds, facilitating oil extraction, and returned as extract to the flask via a siphon arm. This extraction cycle was repeated four times, and the resulting KSO was obtained by evaporating the solvent from the extract under vacuum conditions. Each extraction employed approximately 150 g of crushed seeds and 500 ml of n-hexane. The yield of KSO was approximately 17%, based on the weight of the kapok seeds. The extraction process was repeated multiple times to ensure an adequate quantity of KSO was obtained for the entirety of the experimental runs.

2.3. Epoxidation

The epoxidation was caried out in a jacketed glass reactor with a lid connected to a condenser and equipped with a thermometer to accurately measure the temperature of the reaction mixture. Water, regulated to within ±1 °C accuracy, was circulated through the

Table 1
Epoxidation condition.

#	Variable	Value
1	Formic acid to double bond mole ratio	0.25–1.0
2	Hydrogen peroxide to double bond mole ratio	2
3	Concentration of hydrogen peroxide solution	30%-w
4	Sulfuric acid-to-KSO weight ratio	2%
5	Concentration of sulfuric acid solution	6%-w

jacket. The reactor was placed on top of a magnetic stirrer, and the temperature of the reaction mixture in the reactor was monitored using a thermometer.

A 15 g of KSO sample was placed in the reactor and mixed with an appropriate amount of formic acid and sulfuric acid solution. The mixture was stirred until it became homogeneous, and a determined amount of hydrogen peroxide was added dropwise. The reaction was conducted for 6 h at a controlled temperature of 60 °C. The product was then extracted with n-hexane, washed with distilled water, and dried under vacuum. Further details regarding the epoxidation conditions are provided in Table 1.

2.4. Characterization

KSO and EKSO were characterized by Fourier Transform Infrared (FTIR) and Nuclear Magnetic Resonance (NMR) techniques. FTIR spectra were recorded by a Bruker Alpha spectrophotometer equipped with an OPUS package. The spectra were recorded in the 4000-500 cm^{-1} region with a 4 cm^{-1} resolution. The ^{1}H (500 MHz) and ^{13}C (125 MHz) NMR spectra of KSO and EKSO were recorded on an Agilent NMR spectrometer with DD2 console system and with $CDCl_3$ as a solvent.

2.5. Analysis

The acid value, saponification value, and iodine value were determined according to ISO-660-2020, ISO-3657-2020, and ISO-3961-2018 procedures, respectively. The hydroxyl number was determined according to ASTM D-1957-86. The percentage of oxirane oxygen was determined by the direct method with HBr as outlined in ASTM D-1652-97. The relative fractional conversion to oxirane (RCO), the theoretical maximum oxirane oxygen (OO_T), the overall conversion of double bond (DBC), and the selectivity of the epoxidation reaction towards oxirane oxygen (S) were calculated using equations (1)–(4), respectively [37,38].

$$RCO\ (\%) = 100\ \text{x}\ OO_E\ /\ OO_T \tag{1}$$

$$OO_T\ (\%) = (1600\ \text{x}\ IV_O\ /\ 253.8)\ /\ \{100 + (16\ \text{x}\ IV_O\ /\ 253.8)\} \tag{2}$$

$$DBC\ (\%) = 100\ \text{x}\ (1 - IV_E\ /\ IV_O) \tag{3}$$

$$S\ (\%) = 100\ \text{x}\ RCO\ /\ DBC \tag{4}$$

in these equations, OO_E represents the measured oxirane oxygen, IV_O represents the iodine value of the KSO, and IV_E represents the iodine value of the product.

2.6. Thermal stability test

The thermal stability of PVC was tested both statically and dynamically, using a dehydrochlorination apparatus and a two-roll mill, respectively. These methods were previously described [25]. The dehydrochlorination apparatus consisted of an oil batch provided with a heating tape, a temperature controller, and a 7 mm ID, 1 mm thick glass test tube. Nitrogen gas was used to sweep the hydrogen chloride gas resulting from the degradation in the tube test onto absorbing water at a flow rate of 60 ml min^{-1}. A glass beaker filled with 200 ml of distilled water was placed on a magnetic stirrer to absorb the hydrogen chloride gas. The conductivity of water, which increased due to the absorption of hydrogen chloride, was monitored using a Martini Instrument conductivity meter (model Mi170). The formula of the PVC compound used for the two-roll mill tests can be found in Table 2.

2.7. Mechanical properties measurement

The mechanical properties of the PVC samples in the form of a rectangular bar (100 mm × 10 mm × 0.3 mm) were evaluated using a universal testing machine (Instron 5985). The reported properties include tensile stress, elongation at break, and Young's modulus. The Young's modulus was calculated from the slope of the linear portion of the stress–strain curve in the elastic deformation region. All values were reported as confidence intervals at a 95% confidence level based on at least four samples.

Table 2
Formulation for two-roll mill tests.

#	Additive	Function	Content (phr)
1	Ca/Zn stearate 4/1	Thermal stabilizer	5
2	EKSO	Co-thermal stabilizer	1–4
3	Calcium stearate	Internal lubricant	0.4
4	Stearic acid	Internal lubricant	0.4
5	Paraffin wax	External lubricant	0.6
6	Chlorinated polyethylene	Impact modifier	4
7	Polyacrylic (PA-20)	Processing aid	1
8	Calcium carbonate	Filler	15

2.8. Melt flow index test

Melt flow index (MFI) was measured using an MFI tester of LY-RR model from Guangdong LIYI Technology. The measurement was done according to ASTM D-1238-13 at 190 °C with a 21.6 kg load as recommended by the standard. The measurement was repeated six times with the same formula as for the two-roll mill test.

3. Results and discussion

3.1. Analysis of KSO

The results of the analysis of KSO are shown in Table 3 which also includes data from various sources in the literature. The literature data reveal a broad spectrum of qualities of KSO. The acid value, an indicator of free fatty acids resulting from enzymatic activity during storage and handling of the seeds, ranges from 1.6 to 35.9 mg KOH/g. Oil from fresh seeds typically has a lower acid number, while oil from poorly handled and stored seeds tends to have a higher acid number. The measured acid value of 24.3 mg KOH/g in this work is not as high as the upper limit of the literature range, but still high enough to indicate significant enzymatic activity prior to seed extraction. This is likely due to kapok seed being produced as a waste of processing kapok fiber, and the seeds not being stored properly, often just left in piles around fiber processing facilities. The saponification value, a measure of the quality of raw materials if KSO is to be used as soap, ranges from 129 to 197 mg KOH/g in the literature, with the measured value in this work being 189.4 mg KOH/g, indicating there was still a high amount of triglyceride and fatty acid fractions present. The iodine value is the most important attribute related to epoxidation reaction and provides information on the unsaturation degree in terms of the amount of iodine that can be absorbed per 100 g of sample. The KSO iodine value in the literature is 76.0–130.0 g I_2/100 g, with the measured value in this work of 97.6 g I_2/100 g being approximately in the middle of this range. This value is higher than that of palm oil, which is in the range of 44–58 g I_2/100 g [39], although lower than that of soybean oil, which is in the range of 120–136 g I_2/100 g [39]. The high content of double bonds in KSO makes it an attractive option for use as an epoxy-based co-stabilizer for PVC, particularly since KSO is not commonly used as a food commodity.

3.2. Characteristics of EKSO

Fig. 1 depicts the infrared spectra of KSO and EKSO. The spectra are interpreted by referring to the related infrared spectra in the literature [19,52–55]. The spectrum of KSO exhibits the characteristic absorption bands that are indicative of triglycerides, with the asymmetrical and symmetrical stretching vibration of methylene (-CH_2) located at wave numbers 2922 and 2853 cm^{-1}, respectively. Additionally, the absorption peaks at 1742 and 1711 cm^{-1} show the symmetrical stretching vibrations of (C═O) of ester in triglyceride and carbonyl in free fatty acid, respectively. The noticeable peaks around 1458 and 1163 cm^{-1} correspond to aliphatic CH_2 bending vibration and C–O stretching vibration, respectively. The presence of double bonds is indicated by the absorption peak of C═C–H stretching vibration at 3007 cm^{-1}. The success of epoxidation can be observed through the disappearance of the absorption band of the double bond at 3007 cm^{-1} and the emergence of a new epoxide band in the EKSO spectrum ranging from 844 to 824 cm^{-1}, which is indicative of the formation of the epoxide [38,56,57].

Fig. 2 presents the ^{1}H NMR spectra of KSO and EKSO. When interpreting the spectra, reference was made to related ^{1}H NMR spectra found in the literature [19,53,58]. For the ^{1}H NMR spectrum of KSO, the signals at δ 5.3266–5.3914 ppm corresponds to olefinic protons (-C<u>H</u>═C<u>H</u>-) of unsaturated fatty acids. The signals at δ 5.2454–5.2660 ppm and at δ 4.1153–4.3024 ppm corresponds to the glycerol protons (C<u>H</u>–OCO-R) and (-C<u>H_2</u>-OCO-R), respectively. The signals at δ 2.7429–2.7693 ppm corresponds to linoleyl protons (-CH═CH–C<u>H_2</u>–CH═CH-). The signals around δ 2.3 ppm are due to the second protons of fatty acids (-C<u>H_2</u>-COOH), around δ 2.0 ppm are due to the allylic methylene protons (-C<u>H_2</u>-CH═CH-), at δ 1.5216–1.6028 ppm are due to the third protons of fatty acids (-C<u>H_2</u>-CH_2-COOH), at δ 1.2416–1.2925 ppm are due to the methylene proton ((C<u>H_2</u>)$_n$), and at δ 0.8523–0.8892 ppm indicates the terminal methyl proton (–CH_2–CH_2-CH_2-C<u>H_3</u>). The signal at δ 0.7535 ppm is generated by the cyclopropenic methylene protons of sterculyl and malvalyl [59]. In the ^{1}H NMR spectrum of EKSO, a new signal found at δ 1.4513 ppm represents the methylene protons adjacent to the epoxy group (-C<u>H_2</u>-HCOCH-C<u>H_2</u>-) [60]. In addition, two new groups of signals at δ 1.6709–1.6966 ppm and at δ 3.0289–3.0847 ppm were found. These groups of signals correspond to the methylene protons between two epoxy groups (–HCOCH–C<u>H_2</u>-HCOCH-) and the epoxy protons, respectively [58,60]. The epoxy protons include the epoxy protons derived from oleyl (-<u>H</u>COC<u>H</u>-) and from linoleyl that can be epoxy protons separated by two epoxy groups (-<u>H</u>COCH-CH_2-CHOC<u>H</u>-) or epoxy protons

Table 3
Properties of KSO.

Property	This work	Literature data [Source]
Acid value (mg KOH/g)	24.3 ± 0.2	1.6 [19], 1.7 [40], 4.5 [41], 11.5 [7], 12.0 [9], 13.9 [42], 14.0 [43], 15.4 [10], 16.0 [44], 19.6 [45], 19.8 [46], 21 [47], 21 [14], 28.7 [48], 33.6 [49], 35.9 [50]
Saponification value (mg KOH/g)	189.4 ± 1.1	129.0 [44], 152.8 [41], 172.5 [50], 180.0 [51], 183.0 [40], 186.9 [19], 195 [48], 189–197 [39]
Iodine value (g I_2/100 g)	97.6 ± 2.8	76.0 [51], 94.5 [44], 95.0 [40], 97.7 [7], 101.7 [19], 101.9 [48], 86–110 [39], 130.0 [41]

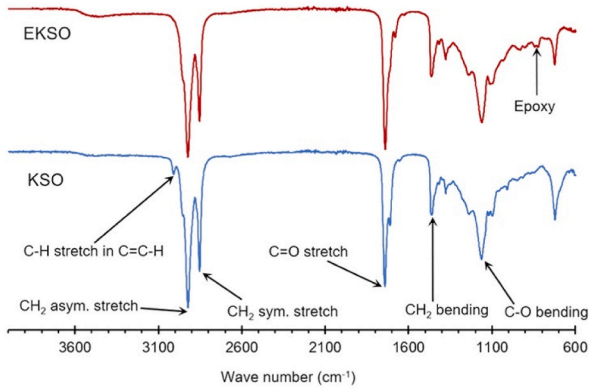

Fig. 1. Infrared spectra of KSO and EKSO.

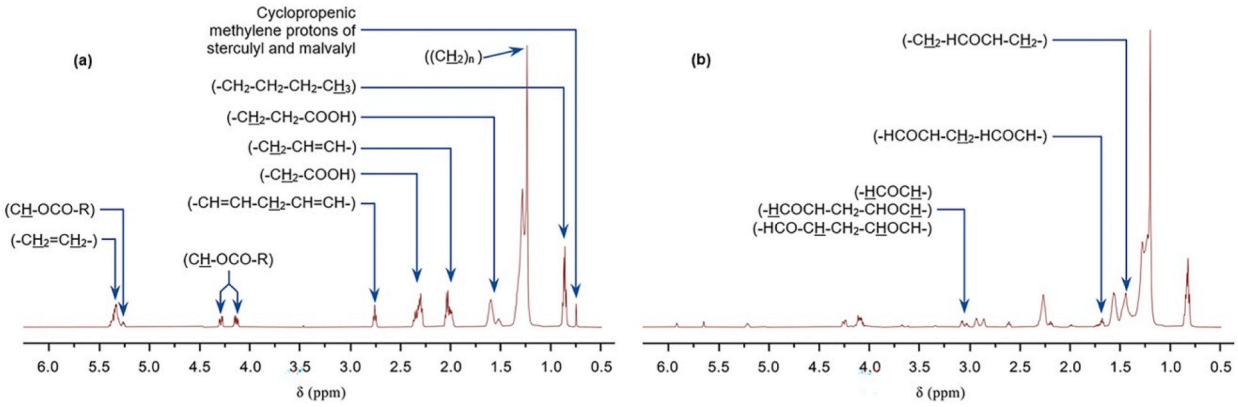

Fig. 2. ^{1}H NMR spectra of KSO (a) and EKSO (b).

separated by a methylene groups (–HCO–CH-CH_2-CHOCH-). The peaks of olefinic protons (-CH═CH-), linoleyl protons (-CH═CH_2–CH_2–CH═CH-), and allylic methylene protons (-CH_2-CH═CH-) disappeared. The peaks of cyclopropenic methylene protons related to the unsaturated bonds of sterculyl and malvalyl also vanished.

Fig. 3 presents the ^{13}C NMR spectra of KSO and EKSO. The interpretation of these spectra was based on reference to corresponding ^{13}C NMR spectra found in the literature [19,53,61,62]. The signals at δ 173.3515–173.4349 ppm and at δ 172.9760 ppm corresponds to the first carbons of triglycerides C1,sn-1,3 and C1,sn-2, respectively. The signals in the δ range of 109.1771–130.2929 ppm correspond to the unsaturated carbons. The peaks at δ 130.0539–130.2929 ppm are due to C9 of linoleyl and linolenyl and C13 of linoleyl, at δ 129.7695–129.8150 ppm are due to C9 and C10 of oleyl, at δ 128.1574–128.1802 ppm are due to C10 of linoleyl and C12

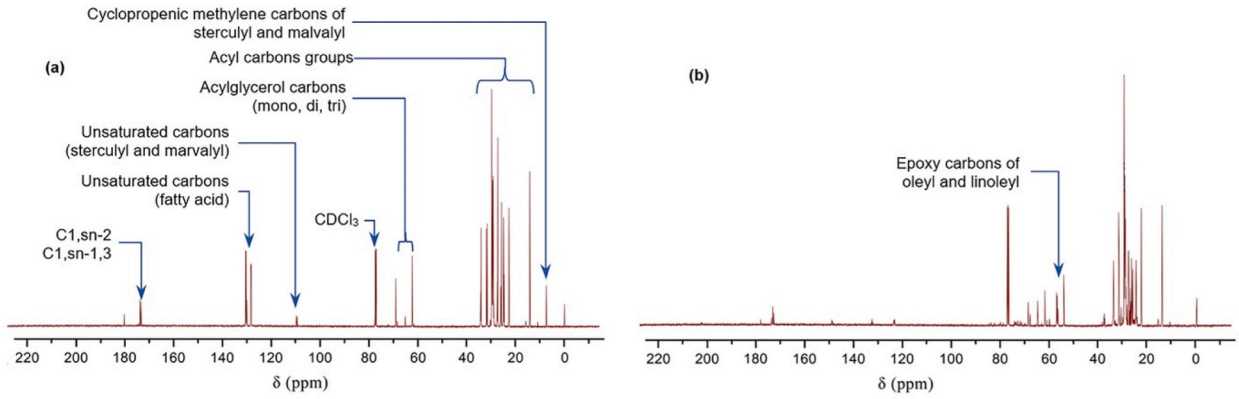

Fig. 3. ^{13}C NMR spectra of KSO (a) and EKSO (b).

and C13 of linolenyl, and at δ 127.9943 is due to C12 of linoleyl and C12 and C15 of linolenyl. The group of signals at δ 109.1771–109.6360 ppm corresponds to the unsaturated carbons of sterculyl and marvalyl [59]. The signals at δ 68.4057–68.9898 ppm and at 65.1171 correspond to the carbons CHO-,sn-2 of triacylglycerol and the carbon CH_2O-,sn-1 of monoacylglycerol, respectively. The signal at δ 62.2041 corresponds to CH_2O-,sn-1,3 of triacylglycerol and CH_2O-,sn-1 of 1,2-diacylglycerol. The signals at δ 34.0939–34.2873 ppm and at δ 31.6360–31.9963 ppm correspond to the C2,sn-2 of all acyl chains and the C16(ω3) of linoleyl, respectively. The signals at δ 29.0036–29.8798 ppm are due to the C4–C7 of all acyl chains, C12–C15 of oleyl, C8–C15 of stearoyl, and C8–C13 of palmitoyl. The signals at 27.3043–27.4902 correspond to the C8 of oleyl and linoleyl and the C11 of oleyl. The signals at 25.7302–26.1323 ppm correspond to the C11 of linoleyl and linolenyl and C14 of linolenyl. The signals at 24.7440–24.9678 ppm, at 22.6920–22.8096 ppm, and at 14.1804–14.2259 ppm correspond to the C3, C17(ω2), and C18(ω1), respectively, of all acyl chains. The peak at 7.4781 ppm represents the cyclopropenic methylene carbons of sterculyl and malvalyl [59]. This signal and the unsaturated signals at δ 128–130 ppm and around δ 109 ppm disappeared in the ^{13}C NMR spectrum of EKSO. New groups of signals, however, appear at δ 56.6179–57.3538 ppm and at δ 54.2738–54.4180 ppm indicating the epoxy carbons of oleyl and linoleyl. The characterizations conducted confirmed that EKSO has been successfully synthesized.

3.3. Analyses of EKSO

Fig. 4 presents the results of the analysis of iodine value, double bond conversion, oxirane oxygen content and selectivity toward EKSO at various mole ratios of formic acid to double bonds. It is evident that EKSO iodine value is much lower than KSO iodine value, indicating that the double bonds have been consumed when subjected to epoxidation reaction. As the mole ratio of formic acid to double bonds increases from 0.25 to 0.5, the EKSO iodine value decreases drastically, while the conversion increases significantly. However, the decline in EKSO iodine value and the increase in conversion rate slowdown in the 0.5–1.0 ratio range, with both values reaching an asymptote at a ratio of formic acid to double bonds of 0.75. Therefore, from the point of view of chemical conversion and additional conversions obtained from the increased use of chemicals, a mole ratio of formic acid to double bonds of 0.5 is considered the optimal ratio.

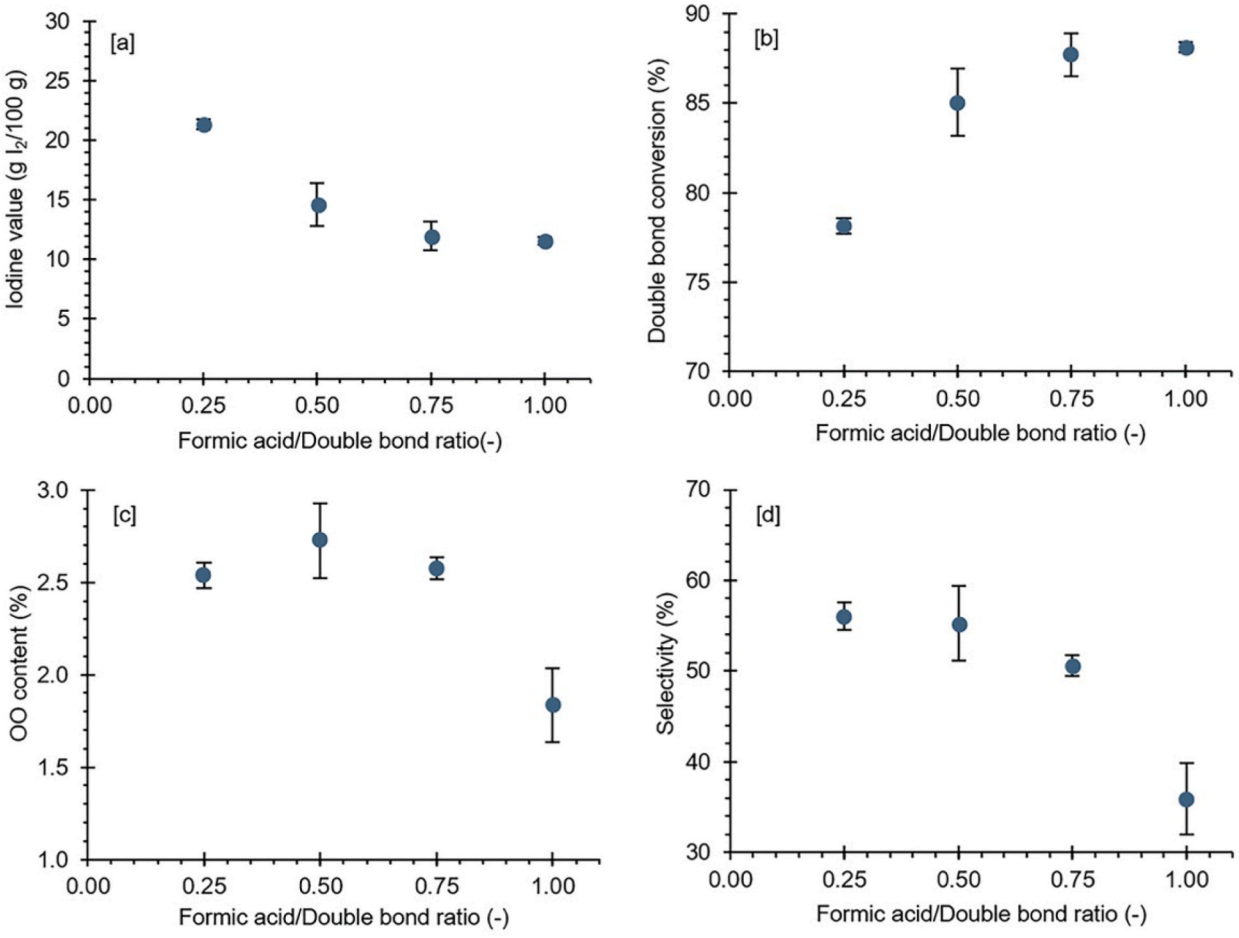

Fig. 4. Acid value (a), double bond conversion (b), oxirane oxygen content (c), and selectivity (d) at various formic acid to doble bond mole ratios.

The maximum oxirane oxygen content of 2.73% is reached when the mole ratio of formic acid to double bonds is 0.5. At this ratio, the selectivity of epoxidation (the conversion of double bonds into epoxide products) was found to be 47%. This indicates that more than half of the double bonds were converted into non-epoxide products, due to epoxy ring opening caused by the presence of peracid, carboxylic acid, water, hydrogen peroxide, and protons. The limits of selectivity due to oxirane ring opening were also found in epoxidizing grape seed oil [63], mustard oil [64], katapang fruit kernel oil [65], and laburnum seed oil [66].

The epoxidation reaction through the formation of peracid in situ using formic acid catalyzed by strong acids occurs through the formation of performic acid in equation (5) and the transfer of oxygen in equation (6) [35,53,67].

$$HCOOH + H_2O_2 \rightleftharpoons HCOO - OH + H_2O \tag{5}$$

$$> C = C < + HCOO - OH \rightarrow > COC < + HCOOH \tag{6}$$

The two side reactions associated with formic acid are represented by equations (7) and (8) [67].

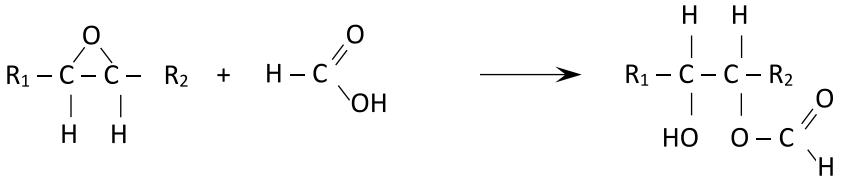

(7)

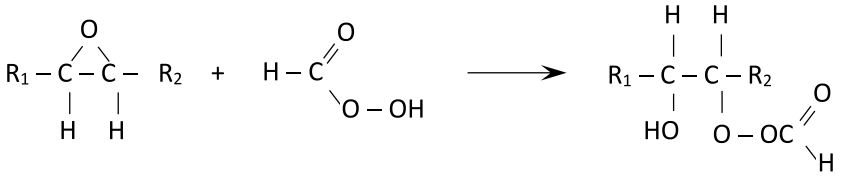

(8)

Formic acid is necessary for the production of performic acid in the reaction (5), but it can also lead to the side reaction (7). Similarly, performic acid is essential for the formation of epoxy through the reaction (6), but it can also cause side reactions that can open epoxy rings through the reaction (8). When the ratio of formic acid to double bonds is low, there is not enough formic acid and performic acid to open the epoxy ring and thus the oxirane number remains low. However, when the ratio of formic acid to double bonds is high, there is enough formic acid and performic acid to be dominant over the epoxy formation, leading to a maximum oxirane oxygen content within the range of formic acid to double bond mole ratios studied.

3.4. Stabilization mechanism

As shown in the literature [30], the stabilizing effects of Ca/Zn stearate are characterized by the synergistic action between the two metal stearates. Zinc stearate imparts a good early color to PVC by substituting labile chlorine atoms according to the reaction in equation (9) [30].

$$PVC - Cl + Zn(OOCR)_2 \rightarrow PVC - OOCR + ZnCl_2 \tag{9}$$

On the other hand, calcium stearate reacts with zinc chloride to recover zinc stearate and to prevent the catalytic effect of zinc chloride through the reaction in equation (10) [30].

$$ZnCl_2 + Ca - (OOCR)_2 \rightarrow Zn(OOCR)_2 + CaCl_2 \tag{10}$$

Additionally, calcium stearate binds hydrogen chloride to form calcium chloride and stearic acid through the reaction in equation (11) [30].

$$Ca - (OOCR)_2 + HCl \rightarrow RCOOH + CaCl_2 \tag{11}$$

The stabilizing mechanism actions of epoxydized oil include binding with hydrogen chloride, substitution of allylic chloride, and formation of complexes with $ZnCl_2$ [30,68]. Epoxides enhance PVC stability by binding any free hydrochloric acid and, in the presence of active zinc ion or cadmium ion, they can substitute labile chlorine atoms in the PVC chain, as shown in equations (12) and (13) [30].

(12)

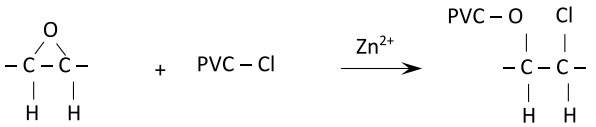

(13)

The complexation of $ZnCl_2$ is described by equations (14) and (15) [68], demonstrating the capability of epoxides to counteract the detrimental effects of $ZnCl_2$.

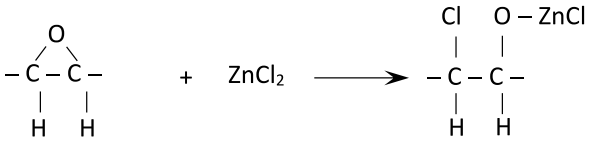

(14)

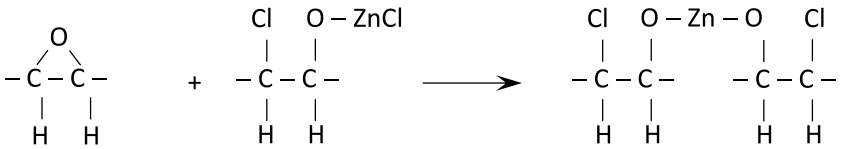

(15)

To confirm the stabilization mechanism outlined above, 1 g of a mixture of PVC resin and thermal stabilizer was placed in a glass tube and then heated in an oil bath at a controlled temperature. Doses of 5 phr and 2 phr were selected for Ca/Zn stearate and EKSO, respectively. Observations were made at 180 °C at various times and with various stabilizers. After a certain heating time, the mixture was removed from the tube, crushed, and sampled for IR spectral measurements. Fig. 5 displays the IR spectra obtained. The spectrum of PVC is characterized by the presence of a C–Cl absorption peak in the wave number range of 605–610 cm^{-1} and the bending vibration band of undegraded CH at a wave number around 1428 cm^{-1}. With the absence of a stabilizer, the intensity of the undegraded CH decreased significantly after 30 min of heating. The spectrum of the PVC resin stabilized by Ca/Zn stearate is characterized by absorption peaks at wave numbers around 1570, 1540, and 1478 cm^{-1}, indicating the presence of COO^{-}. After heating for 15 min, the intensity of these peaks decreased significantly and practically disappeared after 30 min. As the intensity of the COO^{-} vibrational peaks decreases, several new absorption peaks appear, indicating the presence of stabilization products from Ca/Zn stearate. New absorption peaks that appear around wave numbers 3400 and 1630 cm^{-1} are an indication of the presence of calcium dichloride [69]. The existence of a new absorption peak at wave number 1700 cm^{-1} describes the carbonyl group of stearic acid. The intensity of the three absorption peaks increased with the length of the heating time. These phenomena illustrate the performance of calcium stearate

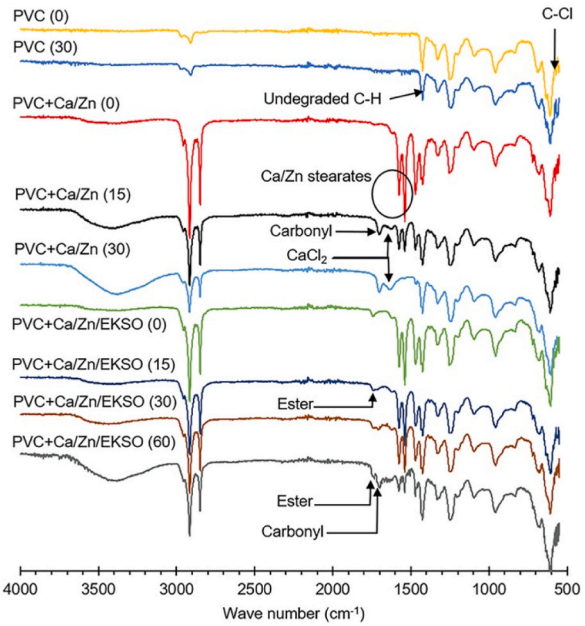

Fig. 5. IR spectra of 180°C-heated PVC (heating times in minutes shown in parentheses).

through the reactions (10) and (11). However, the presence of an ester resulting from the replacement of labile chlorines by zinc stearate through reaction (9) was not found, most likely due to either the small amount of zinc stearate used or because the ester formed reacted with hydrogen chloride and was released from the PVC structure as stearic acid. The quick reduction in the intensity of COO^- vibrational peaks suggests that Ca/Zn stearate is rapidly consumed during heating.

The spectra of PVC resins stabilized by Ca/Zn stearate and EKSO have an absorption peak from the beginning at 1735 cm^{-1} which is related to the presence of ester groups from EKSO itself. This can be confirmed by the fact that the intensity of the peak at that wavelength decreases with increasing heating time, due to EKSO taking part in the stabilization process. Furthermore, if the resin was washed with n-hexane before FTIR analysis, this absorption peak was not observed, either before or after heating. In comparison to PVC stabilized with Ca/Zn stearate without EKSO, the decrease in the COO^- absorption peak is slower when EKSO is present. Even after heating for 60 min, the spectrum of the resin still showed absorption peaks of COO^-, indicating that Ca/Zn stearate was still present. Furthermore, the increase in intensity of the absorption peaks that denote the appearance of stabilization products from calcium stearate is not as rapid as in the resin stabilized with Ca/Zn stearate without EKSO. This implies that the consumption of Ca/Zn stearate is not as fast as when EKSO is absence. This finding further confirms that EKSO effectively binds hydrogen chloride, which reduces the consumption of calcium stearate required to counteract its degrading effects. As a result, more calcium stearate becomes available to recover zinc stearate, improving its efficiency. The roles of the epoxydized group, as evidenced by reactions (14) and (15), are confirmed by the absence of 'zinc burning' in PVC resin containing EKSO. This outcome is attributed to the mitigating effect of epoxides, which counteracts the catastrophic catalytic impact of $ZnCl_2$ in a short period.

3.5. Thermal stability of PVC

Fig. 6 shows the results of dehydrochlorination tests of PVC stabilized with Ca/Zn stearate (5 phr) and EKSO as a co-stabilizer (2 phr) using EKSO synthesized at various mole ratios of formic acid to double bonds, with the corresponding oxirane oxygen contents being extracted from Fig. 4. The shape of the conductivity versus time graphs obtained does not differ from typical dehydrochlorination curves as presented in the literature [70,71]. Initially, the conductivity of water remains stable at its initial value. After a certain time, hydrogen chloride is released, resulting in a significant increase in the conductivity level. Two times as measures of PVC degradation were extracted from the dehydrochlorination curve: the induction time and the stability time. As per literature [22,72], the induction time is the time when hydrogen chloride begins to evolve, taken as the period during which the conductivity increases by 3 μS cm^{-1} and the stability time is the maximum acceptable level of degradation, taken as the period during which the conductivity increases by 50 μS cm^{-1}.

Fig. 7 summarizes the results of the dehydrochlorination tests using EKSO obtained at various formic acid to double bond mole ratios. The mole ratios of formic acid to double bonds give significantly different induction times. The relationship obtained is consistent with the impact on the oxirane oxygen content of the mole ratio of formic acid to double bonds. As with the oxirane oxygen content, the maximum value for the induction time is obtained when EKSO is synthesized at a mole ratio of formic acid to double bonds of 0.5. This corresponds to the role of EKSO in substituting labile chlorines in the PVC structure. The elimination of labile chlorines is closely linked to the initial stability indicated by the induction time. Consequently, the EKSO with the highest oxirane oxygen content yielded the greatest induction time.

There is a tendency for the stability time to decrease with the mole ratio of formic acid to double bonds. EKSO synthesized at a formic acid to double bond mole ratio of 1.0 shows a relatively lower stability time compared to other EKSOs, likely due to its lower oxirane oxygen content. Although the oxirane oxygen content of EKSO synthesized at a formic acid to double bond mole ratio of 0.25 is slightly lower than that at a ratio of 0.5, its stability time is slightly higher. This may be due to the presence of hydroxyl groups, which are formed when the oxirane ring opens and can be measured as the hydroxyl number. The hydroxyl numbers of the EKSOs obtained are presented in Fig. 8. The low oxirane oxygen content indicates that many hydroxyl groups are formed due to the epoxy ring opening. Interestingly, the presence of hydroxyl groups, although contradictory to oxirane oxygen contents, can enhance long-term stability by

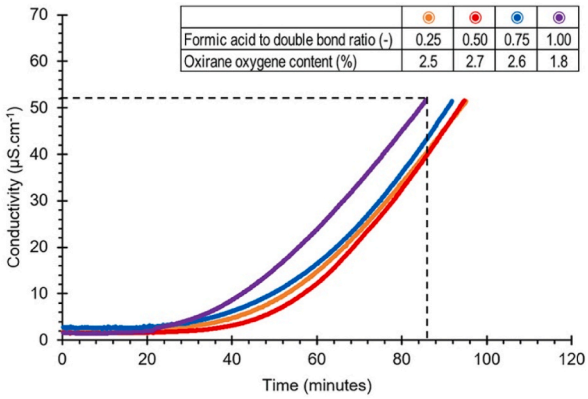

Fig. 6. Dehydrochlorination curves using EKSOs synthesized at various formic acid to double bond mole ratio.

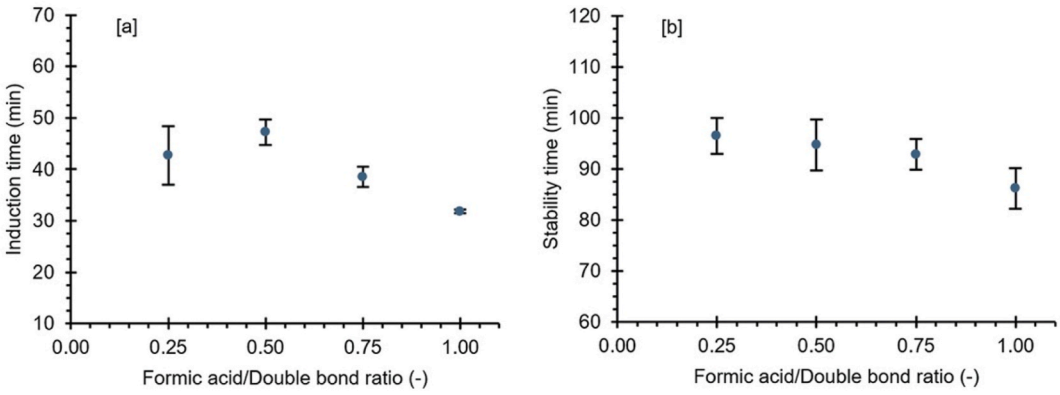

Fig. 7. Induction and stability times using EKSOs synthesized at various formic acid to double bond mole ratio.

scavenging hydrogen chloride, as documented in the literature [22,27,72,73]. Therefore, in addition to calcium stearate and oxirane oxygen, hydroxyl groups formed during the epoxy ring opening of EKSO also contribute to the capture of hydrogen chloride as a degradation product, providing a long-term stabilizing effect for the EKSO. This effect becomes significant when the oxirane oxygen contents are not substantially different, resulting in a lower stability time for EKSO synthesized at the formic acid to double bond mole ratio of 0.5 compared to that synthesized at a ratio of 0.25.

Fig. 9 shows the dehydrochlorination curves of PVC resin stabilized with Ca/Zn (5 phr) stearate in the presence of EKSO at various doses of EKSO, as well as the dehydrochlorination curve of the unstabilized PVC resin. The corresponding induction and stability times are shown in Fig. 10. Without a stabilizer, the induction time is very short (5.6 min), and degradation occurs quickly, resulting in a low stability time of 22.8 min. The addition of Ca/Zn stearate (5 phr) increases the induction time and stability time to 17.8 and 41.6 min, respectively, due to the synergistic effect of the two metal stearates. The effectiveness of EKSO as a co-stabilizer to the Ca/Zn stearate system is evident. When 1 phr of EKSO is added, the induction time is almost doubled compared to Ca/Zn stearate without EKSO, while the stability time increases by almost 1.5 times. This increase in induction and stability times cannot be separated from the stabilization mechanisms provided by EKSO through equations (12) to (15). The effect also results in a decrease in the rate of release of hydrogen chloride with increasing doses of EKSO, as shown by the lowering of the dehydrochlorination curve.

Fig. 10 shows that the stability provided by EKSO increases linearly up to a dose of 4 phr. Further increases in dose from 4 to 8 phr still enhance the stabilizing effect. However, the increase is no longer linear and tends to reach an asymptotic value. Fig. 10 also compares the induction time and stability time between the systems using EKSO and ESBO as co-stabilizers. In the range of doses studied, ESBO provides a longer induction time compared to EKSO, which can be attributed to its higher oxirane oxygen content. The EKSO and ESBO contain oxirane oxygens of 2.7% and 6.1%, respectively. These oxygens replace labile chlorines in the PVC structure, so a higher content delays the release of labile chlorine, thus providing a longer induction time. Although EKSO has a lower oxirane content, it tends to provide a slightly longer stability time, particularly at higher doses. This is also attributed to the presence of hydroxyl groups because of the ring opening. The EKSO used had a hydroxyl number of 76 mg KOH/g, whereas ESBO did not contain any hydroxyl groups. The hydroxyl groups increase long-term stability, which is reflected in the stability time in this case.

The results of roll-mill test for PVC stabilized with Ca/Zn stearate in the presence of EKSO are displayed in Fig. 11. EKSO, which has an oxirane oxygen content of 2.7%, was chosen and its dose was varied in the range of 0–4 phr. The doses for the other additives were set according to Table 2. Unstabilized PVC and PVC stabilized with Ca/Zn stearate in the presence of ESBO were used for comparison.

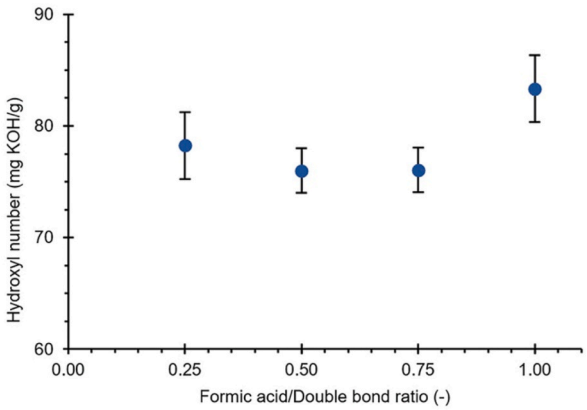

Fig. 8. Hydroxyl number of EKSO.

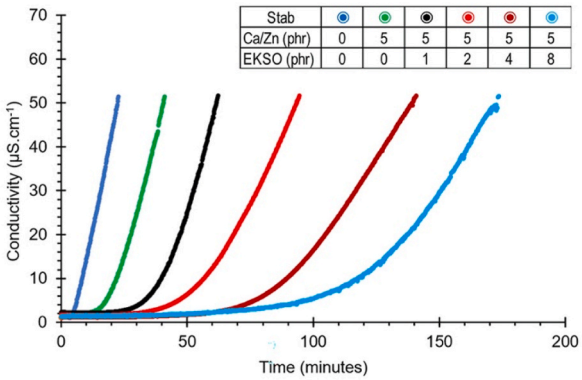

Fig. 9. Dehydrochlorination curves at various doses of EKSO.

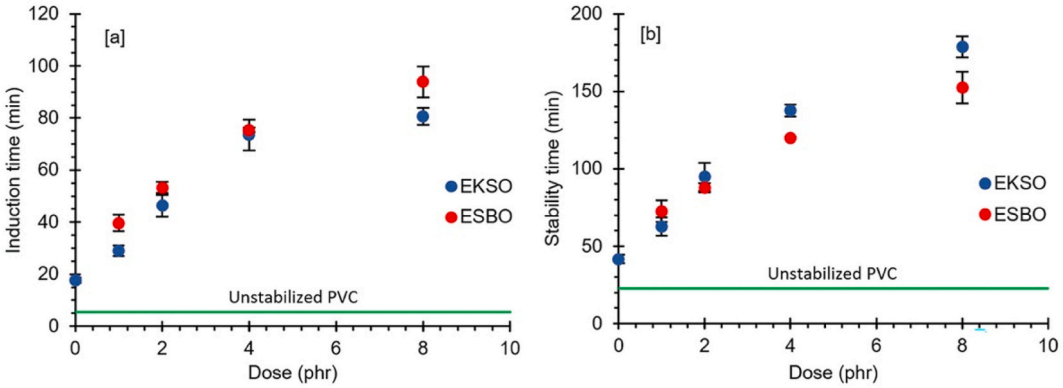

Fig. 10. Induction time (a) and stability time (b) from dehydrochlorination tests at various doses of co-stabilizers.

The tests were conducted at 180 °C and 190 °C.

It can be observed that the unstabilized PVC quickly turns dark. At 180 °C, the performance difference between the Ca/Zn stearate system with and without EKSO is not distinct until 110 min. At 120 min, the PVC stabilized with Ca/Zn stearate without EKSO begins to take on a brownish color, like that of the unstabilized PVC. In contrast, the PVC stabilized with EKSO in the presence of Ca/Zn stearate

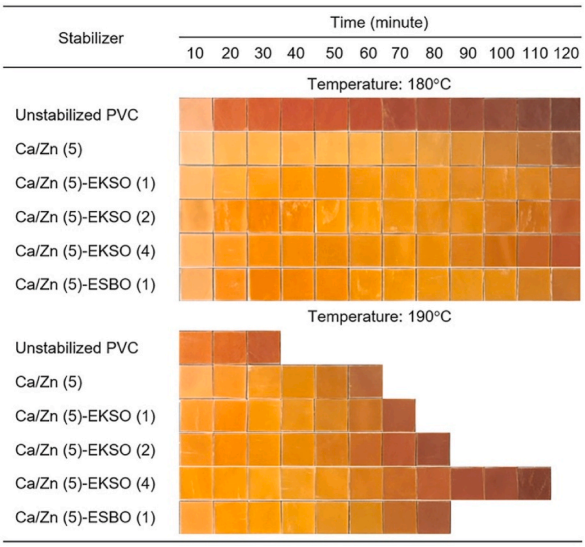

Fig. 11. Discoloration from roll mill tests, doses in phr are shown in parenthesis.

remains non-brownish until the 120th minute, indicating that EKSO delayed the degradation of PVC.

The effect of the EKSO dose on the color change at 180 °C for 120 min is not particularly noticeable. All doses were able to prevent dark brown coloration in the PVC, indicating that the PVC was not burned. The effect of adding EKSO is more pronounced at a higher temperature. At 190 °C, unstabilized PVC became brittle and could not be rolled after 30 min. The PVC stabilized with 5 phr of Ca/Zn stearate, turned brown after 60 min and became brittle, unable to be rolled. EKSO extended the stability of PVC by 10–30 min compared to Ca/Zn stearate without EKSO for doses in the range of 1–4 phr.

The results using EKSO at more than 1 phr appear slightly darker than those using ESBO and Ca/Zn stearate without EKSO, likely due to the thermal oxidation of impurities in the KSO. It is noteworthy that the KSO used in this study was crude, containing impurities such as wax and gum. The tests conducted, however, have shown that EKSO, as a co-stabilizer, can enhance the thermal stability of PVC.

3.6. Mechanical properties of PVC

PVC is a polymer with properties that can be modified by adding additives. Commonly modified properties include flexibility and ductility, which can be changed by using plasticizers. Epoxidized vegetable oil is a popular plasticizer [74–77]. Therefore, it is important to examine the effect of using EKSO as a thermal stabilizer on the mechanical properties of PVC. Table 4 shows the mechanical properties of PVC films with various doses of EKSO. Additionally, the mechanical properties of PVC films stabilized by Ca/Zn in the absence of a co-stabilizer and in the presence of ESBO are also presented. Tensile strength measures the material's resistance to an applied tensile load, strain at break assesses the flexibility or ductility of a material, and Young's modulus evaluates the ease with which a material undergoes deformation under an applied load [78].

Comparative t-tests were conducted at a 95% confidence level, using the Ca/Zn (4/1, 5 phr) data as a reference. The results showed P-values ranging from 0.000 to 0.022 for EKSO and 0.000 to 0.043 for ESBO as co-stabilizers. These findings indicate that the observed differences are statistically significant. The inclusion of EKSO in the Ca/Zn stearate system leads to a decrease in tensile strength, while increasing strain and Young's modulus. As a result, the plasticity of PVC increases when EKSO is used. The impact of increasing plasticity depends on the dosage applied. At low doses (1–2 phr), the table shows that adding EKSO reduces tensile stress by a maximum of 22% compared to when no co-stabilizer is present. However, it still improves the thermal stability of the PVC resin. A similar effect is observed when ESBO is used as a co-stabilizer.

Comparative tests between EKSO and ESBO at 2 and 4 phr result in P-values ranging from 0.010 to 0.028, 0.578 to 0.678, and 0.047 to 0.35 for tensile stress, Young's modulus, and elongation at break, respectively. These results suggest that the observed differences in Young's modulus and elongation at break lack statistical significance. However, the differences in tensile stress are found to be significant, indicating that EKSO lowers tensile strength more than ESBO. This effect might be attributed to the presence of saturated fatty acids. As mentioned earlier, the iodine value of KSO is significantly lower than that of soybean oil. Consequently, it contains saturated fatty acids that do not undergo epoxidation. In the formulation, these saturated fatty acids act as internal lubricants, which tend to soften the PVC.

3.7. Flowability of PVC

Flowability is a critical factor affecting the overall processability of PVC. Understanding the impact of new additives on flowability is essential. One simple measure of flowability is MFI [79,80]. Fig. 12 presents the MFI results for PVC at various doses of EKSO used as a co-stabilizer, measured at 190 °C with a 21.6 kg load. ESBO is also included for comparison.

Without a co-stabilizer, using Ca/Zn stearate at 5 phr gives an MFI of 5.5 $\pm$ 0.5 g/10 min. At lower doses (less than 2 and 4 phr for EKSO and ESBO, respectively), the MFI was a little bit smaller, indicating that the involvement of the two epoxidized oils increase the melt viscosity, thus reduced flowability. This is attributed to the co-stabilizing effect of the epoxy groups. As discussed earlier, epoxy, as a co-stabilizer, can enter the PVC structure, replacing the allylic chloride, and form complexes with $ZnCl_2$. Both actions result in increased molecular weight, leading to higher viscosity and reduced flowability. As stated in the literature [81,82], MFI is inversely proportional to the molecular weight, meaning that the higher the molecular weight, the lower the MFI, and vice versa.

At doses above 2 phr, the addition of EKSO sharply increase the MFI, suggesting the appearance of a plasticizing effect. Similarly, ESBO significantly increase the MFI at doses above 4 phr. These observations align with the results of the mechanical property measurements, where both EKSO and ESBO showed a significant decrease in tensile strength starting at doses of 2 and 4 phr, respectively. At the same doses, EKSO showed a higher MFI when compared to ESBO, possibly attributed to the presence of unepoxidized saturated fatty acids in EKSO. Fatty acids have internal lubricant effects [83,84] and internal lubricants reduce melt viscosity [85,86]. Internal lubricants help lower the intermolecular forces between PVC particles, making it easier for them to move closer and adhere to each other. This results in improved fusion leading to a better flowability.

4. Conclusions

EKSO has been synthesized using performic acid, formed in situ in the presence of sulfuric acid as a catalyst. The formic acid to double bond mole ratio was varied in the range of 0.25–1.00. The completion of the reaction was confirmed by FTIR and NMR spectral analysis. A maximum oxirane oxygen content of 2.7% in the synthesized EKSO was obtained at a formic acid to double bond mole ratio of 0.5. The application of EKSO as a co-stabilizer in the presence of Ca/Zn stearate for stabilizing PVC has also been studied. Both static and dynamic tests showed that the addition of EKSO in the Ca/Zn stearate system results in a significant increase in thermal stability

Table 4
Mechanical properties of PVC.

Stabilizer	Tensile stress (MPa)	Young's modulus (MPa)	Elongation at break (%)
Ca/Zn (4/1, 5 phr)	31.5 ± 2.3	11.4 ± 1.1	5.9 ± 1.9
Ca/Zn-EKSO (1 phr)	27.6 ± 1.6	13.1 ± 1.1	9.1 ± 1.4
Ca/Zn-EKSO (2 phr)	24.7 ± 0.4	13.2 ± 1.5	9.3 ± 1.2
Ca/Zn-EKSO (4 phr)	23.1 ± 1.3	14.7 ± 1.8	11.9 ± 2.2
Ca/Zn-ESBO (2 phr)	26.1 ± 1.5	13.6 ± 2.5	9.9 ± 1.5
Ca/Zn-ESBO (4 phr)	25.0 ± 1.0	15.3 ± 2.7	13.0 ± 1.3

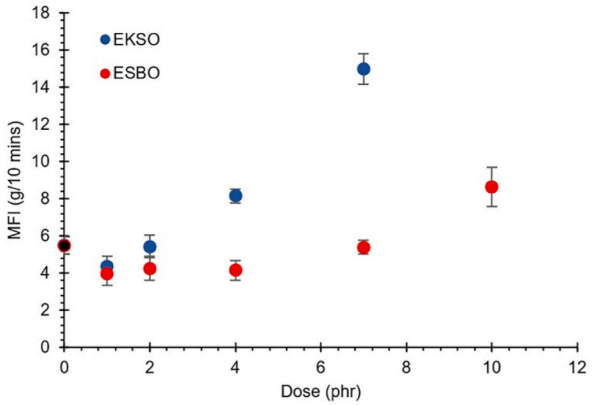

Fig. 12. MFI of PVC.

for PVC. The efficacy of EKSO as a co-stabilizer is also quite competitive with ESBO. Measuring the mechanical properties showed that the use of EKSO reduces the strength of PVC due to an increase in plasticity. However, the decrease in strength experienced is not that great due to the use of small doses. On the other hand, when utilizing small doses (<2 phr), there is a tendency for flowability to decrease, but the reduction is not significant either. Overall, these findings suggest that EKSO could be a useful co-stabilizer for PVC in industrial applications.

Author contribution statement

I Dewa Gede Arsa Putrawan: Conceived and designed the experiments; Performed the experiments; Analyzed and interpreted the data; Contributed reagents, materials, analysis tools or data; Wrote the paper. Adli Azharuddin: Performed the experiments; Analyzed and interpreted the data. Jumrawati Jumrawati: Performed the experiments.

Data availability statement

Data included in article/supp. Material/referenced in article.

Additional information

No additional information is available for this paper.

Funding statement

This work is supported by Institut Teknologi Bandung (ITB) research grant under PPMI 2022 Program.

Declaration of competing interest

The authors declare that they have no known competing financial interests or personal relationships that could have appeared to influence the work reported in this paper.

Acknowledgements

The PVC resins provided by Asahi Chemical Indonesia Company are greatly appreciated.

References

[1] C.S. Quek, N. Ngadi, M.A. Ahmad Zaini, The oil-absorbing properties of kapok fiber – a commentary, J. Taibah Univ. Sci. 14 (1) (2020) 507–512, https://doi.org/10.1080/16583655.2020.1747767.

[2] X. Gómez-Maqueo, A. Gamboa-deBuen, The biology of the genus ceiba, a potential source for sustainable production of natural fiber, Plants 11 (4) (2022) 521, https://doi.org/10.3390/plants11040521.

[3] R.H. Sangalang, Kapok fiber- structure, characteristics and applications: a review, orient, J. Chem. 37 (3) (2021) 513–523, https://doi.org/10.13005/ojc/370301.

[4] Analytic Research Consulting, Kapok Fiber Market, 2022. https://www.industryarc.com/Research/Global-Kapok-Fiber-Market-Research-511498, 11.21.22.

[5] A.M. Lykke, S.B. Gregersen, E.A. Padonou, I.H.N. Bassolé, T.K. Dalsgaard, Potential of unconventional seed oils and fats from west african trees: a review of fatty acid composition and perspectives, Lipids 56 (4) (2021) 357–390, https://doi.org/10.1002/lipd.12305.

[6] S. Krist, Vegetable Fats and Oils, Springer, Switzerland, 2020.

[7] K.W. Cheah, S. Yusup, L.F. Chuah, A. Bokhari, Physio-chemical studies of locally sourced non-edible oil: prospective feedstock for renewable diesel production in Malaysia, Procedia Eng. 148 (2016) 451–458, https://doi.org/10.1016/j.proeng.2016.06.460.

[8] D.-F. Hwang, T.-Y. Chen, Toxins in Food: Naturally Occurring in *Encyclopedia Of Food And Health*, Academic Press, Oxford, 2016, https://doi.org/10.1016/B978-0-12-384947-2.00698-X.

[9] H.C. Ong, A.S. Silitonga, H.H. Masjuki, T.M.I. Mahlia, W.T. Chong, M.H. Boosroh, Production and comparative fuel properties of biodiesel from non-edible oils: jatropha curcas, Sterculia foetida and Ceiba pentandra, Energy Convers. Manag. 73 (2013) 245–255, https://doi.org/10.1016/j.enconman.2013.04.011.

[10] H.C. Ong, J. Milano, A.S. Silitonga, M.H. Hassan, A.H. Shamsuddin, C.-T. Wang, T.M. Indra Mahlia, J. Siswantoro, F. Kusumo, J. Sutrisno, Biodiesel production from Calophyllum inophyllum-Ceiba pentandra oil mixture: optimization and characterization, J. Clean. Prod. 219 (2019) 183–198, https://doi.org/10.1016/j.jclepro.2019.02.048.

[11] S. Bakthavathsalam, R.I. Gounder, K. Muniappan, The influence of ceramic-coated piston crown, exhaust gas recirculation, compression ratio and engine load on the performance and emission behavior of kapok oil–diesel blend operated diesel engine in comparison with thermal analysis, Environ. Sci. Pollut. Res. 26 (24) (2019) 24772–24794, https://doi.org/10.1007/s11356-019-05678-x.

[12] L.F. Chuah, A. Bokhari, S. Yusup, J.J. Klemeš, M.M. Akbar, S. Saminathan, Optimization on pretreatment of kapok seed (Ceiba pentandra) oil via esterification reaction in an ultrasonic cavitation reactor, Biomass Convers. Biorefinery 7 (1) (2017) 91–99, https://doi.org/10.1007/s13399-016-0207-9.

[13] C. Nandakumar, V. Raman, C.G. Saravanan, M. Vikneswaran, S. Prasanna Raj Yadav, M. Thirunavukkarasu, Effect of nozzle hole geometry on the operation of kapok biodiesel in a diesel engine, Fuel 276 (2020), 118114, https://doi.org/10.1016/j.fuel.2020.118114.

[14] S. Pooja, B. Anbarasan, V. Ponnusami, A. Arumugam, Efficient production and optimization of biodiesel from kapok (Ceiba pentandra) oil by lipase transesterification process: addressing positive environmental impact, Renew. Energy 165 (2021) 619–631, https://doi.org/10.1016/j.renene.2020.11.053.

[15] K. Udhayakumar, P. Sakthivel, V. Suresh, K.K. Kavin, P. Paramadhayalan, Experimental investigation of performance of single cylinder DI diesel engine fueled with diesel and Kapok seed oil, Int. Conf. Mater. Manuf. Mech. Eng. Sustain. Dev. 46 (2021) 3739–3742, https://doi.org/10.1016/j.matpr.2021.02.012.

[16] A. Hameed, A. Mukhtar, U. Shafiq, M. Qizilbash, M.S. Khan, T. Rashid, C.B. Bavoh, W.U. Rehman, A. Guardo, Experimental investigation on synthesis, characterization, stability, thermo-physical properties and rheological behavior of MWCNTs-kapok seed oil based nanofluid, J. Mol. Liq. 277 (2019) 812–824, https://doi.org/10.1016/j.molliq.2019.01.012.

[17] A. Mukhtar, S. Saqib, F. Safdar, A. Hameed, S. Rafiq, N.B. Mellon, R. Amen, M.S. Khan, S. Ullah, M.A. Assiri, M. Babar, M.A. Bustam, W.U. Rehman, Z.M. A. Merican, Experimental and comparative theoretical study of thermal conductivity of MWCNTs-kapok seed oil-based nanofluid, Int. Commun. Heat Mass Tran. 110 (2020), 104402, https://doi.org/10.1016/j.icheatmasstransfer.2019.104402.

[18] S. Shankar, M. Manikandan, D.K. Karupannasamy, C. Jagadeesh, A. Pramanik, A.K. Basak, Investigations on the tribological behaviour, toxicity, and biodegradability of kapok oil bio-lubricant blended with (SAE20W40) mineral oil, Biomass Convers. Biorefinery 13 (5) (2021) 3669–3681, https://doi.org/10.1007/s13399-021-01394-0.

[19] F. Anwar, U. Rashid, S.A. Shahid, M. Nadeem, Physicochemical and antioxidant characteristics of kapok (ceiba pentandra gaertn.) seed oil, J. Am. Oil Chem. Soc. 91 (6) (2014) 1047–1054, https://doi.org/10.1007/s11746-014-2445-y.

[20] Y. Guo, F. Leroux, W. Tian, D. Li, P. Tang, Y. Feng, Layered double hydroxides as thermal stabilizers for Poly(vinyl chloride): a review, Appl. Clay Sci. 211 (2021), 106198, https://doi.org/10.1016/j.clay.2021.106198.

[21] C. Jubsilp, A. Asawakosinchai, P. Mora, D. Saramas, S. Rimdusit, Effects of organic based heat stabilizer on properties of polyvinyl chloride for pipe applications: a comparative study with Pb and CaZn systems, Polymers 14 (1) (2021) 133, https://doi.org/10.3390/polym14010133.

[22] Y. Li, D. Li, W. Han, M. Zhang, B. Ai, L. Zhang, H. Sun, Z. Cui, Facile synthesis of di-mannitol adipate ester-based zinc metal alkoxide as Bi-functional additives for poly(vinyl chloride), Polymers 11 (5) (2019) 813, https://doi.org/10.20944/preprints201904.0006.v1.

[23] M. Wang, T. Wu, Q. Bu, X. Song, M. Li, S. Yuan, Rare earth Ce based metal organic framework as efficient synergistic thermal stabilizer for PVC: preparation and thermal stabilization behavior, Thermochim. Acta 718 (2022), 179365, https://doi.org/10.1016/j.tca.2022.179365.

[24] F. Ye, Q. Ye, H. Zhan, Y. Ge, X. Ma, X. Wang, Synthesis and study of zinc orotate and its synergistic effect with commercial stabilizers for stabilizing poly(vinyl chloride), Polymers 11 (2) (2019) 194, https://doi.org/10.3390/polym11020194.

[25] I.D.G.A. Putrawan, A. Indarto, Y. Octavia, Thermal stabilization of polyvinyl chloride by calcium and zinc carboxylates derived from byproduct of palm oil refining, Heliyon 8 (6) (2022), e10079, https://doi.org/10.1016/j.heliyon.2022.e10079.

[26] M. Xue, Y. Lu, K. Li, B. Wang, Y. Lu, Thermal characterization and kinetic analysis of polyvinyl chloride containing Sn and Zn, J. Therm. Anal. Calorim. 139 (2) (2019) 1479–1492, https://doi.org/10.1007/s10973-019-08505-0.

[27] M. Zhang, W. Han, X. Hu, D. Li, X. Ma, H. Liu, L. Liu, W. Lu, S. Liu, Pentaerythritol p-hydroxybenzoate ester-based zinc metal alkoxides as multifunctional antimicrobial thermal stabilizer for PVC, Polym. Degrad. Stabil. 181 (2020), 109340, https://doi.org/10.1016/j.polymdegradstab.2020.109340.

[28] A.M.A. El-Ghaffar, E.A.M. Youssef, M.F. Afify, High performance metal stearates thermal stabilizers for poly vinyl chloride, Int. J. Petrochem. Sci. Eng. 4 (4) (2019) 162–168.

[29] N.T. Thuy, V.M. Duc, N.T. Liem, The epoxidized vietnam rubber seed oil as a secondary plasticizer/thermal stabilizer in PVC processing, Int. J. Polym. Sci. 2021 (2021), 5525547, https://doi.org/10.1155/2021/5525547.

[30] M. Schiller, PVC Additives: Performance, Chemistry, Development, and Sustainability, Carl Hanser Verlag, Munich, 2015.

[31] M.T. Benaniba, N. Belhaneche-Bensemra, G. Gelbard, Stabilization of PVC by epoxidized sunflower oil in the presence of zinc and calcium stearates, Polym. Degrad. Stabil. 82 (2) (2003) 245–249, https://doi.org/10.1016/s0141-3910(03)00178-2.

[32] M.T. Benaniba, N. Belhaneche-Bensemra, G. Gelbard, Stabilizing effect of epoxidized sunflower oil on the thermal degradation of poly(vinyl chloride), Polym. Degrad. Stabil. 74 (3) (2001) 501–505, https://doi.org/10.1016/S0141-3910(01)00170-7.

[33] M.T. Taghizadeh, N. Nalbandi, A. Bahadori, Stabilizing effect of epoxidized sunflower oil as a secondary stabilizer for Ca/Hg stabilized PVC, Express Polym. Lett. 2 (1) (2008) 65–76.

[34] T.O. Egbuchunam, D. Balköse, F.E. Okieimen, Effect of zinc soaps of rubber seed oil (RSO) and/or epoxidized rubber seed oil (ERSO) on the thermal stability of PVC plastigels, Polym. Degrad. Stabil. 92 (8) (2007) 1572–1582, https://doi.org/10.1016/j.polymdegradstab.2007.05.002.

[35] Y. Ji, L. Xu, Q. Xu, X. Liu, S. Lin, S. Liao, W. Wang, D. Lan, Synthesis and characterization of epoxidized silkworm pupae oil and its application as polyvinyl chloride, Appl. Biochem. Biotechnol. 194 (3) (2022) 1290–1302, https://doi.org/10.1007/s12010-021-03715-5.

[36] M. Rozina, M. Ahmad, M. Zafar Alruqi, Cleaner production of biodiesel from novel and non-edible seed oil of Chamaerops humilis using recyclable cobalt oxide nanoparticles: a contribution to resilient and sustainable world, J. Clean. Prod. 369 (2022), 133378, https://doi.org/10.1016/j.jclepro.2022.133378.

[37] I. Dominguez-Candela, A. Lerma-Canto, S.C. Cardona, J. Lora, V. Fombuena, Physicochemical characterization of novel epoxidized vegetable oil from chia seed, Oil., Mater. Basel Switz. 15 (9) (2022) 3250, https://doi.org/10.3390/ma15093250.

[38] A.H. Suzuki, B.G. Botelho, L.S. Oliveira, A.S. Franca, Sustainable synthesis of epoxidized waste cooking oil and its application as a plasticizer for polyvinyl chloride films, Eur. Polym. J. 99 (2018) 142–149, https://doi.org/10.1016/j.eurpolymj.2017.12.014.

[39] A. Thomas, B. Matthäus, H.-J. Fiebig, Fats and Fatty Oils in *Ullmann's Encyclopedia Of Industrial Chemistry*, Wiley-VCH Verlag GmbH & Co. KGaA, Weinheim, Germany, 2015, https://doi.org/10.1002/14356007.a10_173.pub2.

[40] S.K. Berry, The characteristics of the kapok (ceiba pentadra, gaertn.) seed oil, Pertanika 2 (1) (1979) 1–4.

[41] P.S. Montcho, L. Tchiakpe, G. Nonviho, F.T.D. Bothon, A. Sidohounde, C.P.A. Dossa, D. Bessieres, A. Chrostowska, D.C.K. Sohounhloue, Fatty acid profile and quality parameters of Ceiba pentandra (L.) seed oil: a potential source of biodiesel, J. Pet. Technol. Altern. Fuels 9 (3) (2018) 14–19, https://doi.org/10.5897/JPTAF2018.0141.

[42] T. Lieu, S. Yusup, M. Moniruzzaman, Kinetic study on microwave-assisted esterification of free fatty acids derived from Ceiba pentandra Seed Oil, Bioresour. Technol. 211 (2016) 248–256, https://doi.org/10.1016/j.biortech.2016.03.105.

[43] M. Balajii, S. Niju, Banana peduncle – a green and renewable heterogeneous base catalyst for biodiesel production from Ceiba pentandra oil, Renew. Energy 146 (2020) 2255–2269, https://doi.org/10.1016/j.renene.2019.08.062.

[44] C. Muhammad, Biodiesel production from *Ceiba pentandra* seed oil using CaO derived from snail shell as catalyst, Pet. Sci. Eng. 2 (1) (2018) 7, https://doi.org/10.11648/j.pse.20180201.12.

[45] R.D. Kusumaningtyas, Haifah, D. Widjanarko, H. Prasetiawan, Y.W.P. Budiono, A.D.H. Kusuma, N.D. Anggraeni, S.C.F. Kurnita, Experimental and kinetic study of free fatty acid esterification derived from Ceiba pentandra seed oil with ethanol, J. Phys. Conf. Ser. (3) (2021), 032022, https://doi.org/10.1088/1742-6596/1918/3/032022, 1918.

[46] L.K. Ong, C. Effendi, A. Kurniawan, C.X. Lin, X.S. Zhao, S. Ismadji, Optimization of catalyst-free production of biodiesel from Ceiba pentandra (kapok) oil with high free fatty acid contents, Energy 57 (2013) 615–623, https://doi.org/10.1016/j.energy.2013.05.069.

[47] T. Senthil Kumar, P. Senthil Kumar, K. Annamalai, Experimental study on the performance and emission measures of direct injection diesel engine with Kapok methyl ester and its blends, Renew. Energy 74 (2015) 903–909, https://doi.org/10.1016/j.renene.2014.09.022.

[48] P. Sivakumar, S. Sindhanaiselvan, N.N. Gandhi, S.S. Devi, S. Renganathan, Optimization and kinetic studies on biodiesel production from underutilized Ceiba Pentandra oil, Fuel 103 (2013) 693–698, https://doi.org/10.1016/j.fuel.2012.06.029.

[49] A.S. Silitonga, H.C. Ong, T.M.I. Mahlia, H.H. Masjuki, W.T. Chong, Biodiesel conversion from high FFA crude jatropha curcas, Calophyllum inophyllum and ceiba pentandra oil, Energy Proc. 61 (2014) 480–483, https://doi.org/10.1016/j.egypro.2014.11.1153.

[50] N.A. Handayani, H. Santosa, M. Sofyan, I. Tanjung, A. Chyntia, P.A.R.S. Putri, Z.R. Ramadhan, Biodiesel production from kapok (ceiba pentandra) seed oil using naturally alkaline catalyst as an effort of green energy and technology, Int. J. Renew. Energy Dev. 2 (3) (2013) 169–173, https://doi.org/10.14710/ijred.2.3.169-173.

[51] K. Anigo, B. Dauda, A. Sallau, I. Chindo, Chemical composition of kapok (ceibapentandra) seed and physicochemical properties of its oil, Niger, J. Basic Appl. Sci. 21 (2) (2013) 105–108, https://doi.org/10.4314/njbas.v21i2.3.

[52] F. Ashine, S. Balakrishnan, Z. Kiflie, B.Z. Tizazu, Epoxidation of Argemone mexicana oil with peroxyacetic acid formed in-situ using sulfated tin (IV) oxide catalyst: characterization; kinetic and thermodynamic analysis, Heliyon 9 (1) (2023), e12817, https://doi.org/10.1016/j.heliyon.2023.e12817.

[53] D. Favero, V.R.R. Marcon, T. Barcellos, C.M. Gómez, M.J. Sanchis, M. Carsí, C.A. Figueroa, O. Bianchi, Renewable polyol obtained by microwave-assisted alcoholysis of epoxidized soybean oil: preparation, thermal properties and relaxation process, J. Mol. Liq. 285 (2019) 136–145, https://doi.org/10.1016/j.molliq.2019.04.078.

[54] P.P. Lankhorst, A.-N. Chang, The Application of NMR in Compositional and Quantitative Analysis of Oils and Lipids in *Modern Magnetic Resonance*, Springer International Publishing, Cham, Switzerland, 2017, https://doi.org/10.1007/978-3-319-28275-6_108-1.

[55] A. Rohman, Infrared spectroscopy for quantitative analysis and oil parameters of olive oil and virgin coconut oil: a review, Int. J. Food Prop. 20 (7) (2016) 1447–1456, https://doi.org/10.1080/10942912.2016.1213742.

[56] D. Derawi, J. Salimon, Optimization on epoxidation of palm olein by using performic acid, E-J. Chem. 7 (4) (2010) 1440–1448, https://doi.org/10.1155/2010/384948.

[57] D.R. Sawitri, P. Mulyono, R. Rochmadi, A. Budiman, Chemical epoxidation of oleic acid to produce AB type monomer for fatty-acid-based polyester synthesis, J. Teknol. 83 (6) (2021) 157–166, https://doi.org/10.11113/jurnalteknologi.v83.16912.

[58] W. Xia, S.M. Budge, M.D. Lumsden, 1H-NMR characterization of epoxides derived from polyunsaturated fatty acids, J. Am. Oil Chem. Soc. 93 (4) (2016) 467–478, https://doi.org/10.1007/s11746-016-2800-2.

[59] S. Rosselli, R. Tundis, M. Bruno, M. Leporini, T. Falco, R. Gagliano Candela, N. Badalamenti, M.R. Loizzo, Ceiba speciosa (A. St.-Hil.) seeds oil: fatty acids profiling by GC-MS and NMR and bioactivity, Molecules 25 (5) (2020) 1037, https://doi.org/10.3390/molecules25051037.

[60] J.F. Nieto, E.V. Santiago, S.H. López, Determination of the number of epoxides groups by FTIR-HATR and its correlation with 1H NMR, in epoxidized linseed oil, Adv. Anal. Chem. 11 (1) (2021) 1–8.

[61] M.E. Di Pietro, A. Mannu, A. Mele, NMR determination of free fatty acids in vegetable oils, Processes 8 (4) (2020) 410, https://doi.org/10.3390/pr8040410.

[62] R. Popescu, D. Costinel, O.R. Dinca, A. Marinescu, I. Stefanescu, R.E. Ionete, Discrimination of vegetable oils using NMR spectroscopy and chemometrics, Food Control 48 (2015) 84–90, https://doi.org/10.1016/j.foodcont.2014.04.046.

[63] J.C. de Haro, I. Izarra, J.F. Rodríguez, Á. Pérez, M. Carmona, Modelling the epoxidation reaction of grape seed oil by peracetic acid, J. Clean. Prod. 138 (2016) 70–76, https://doi.org/10.1016/j.jclepro.2016.05.015.

[64] P.D. Jadhav, A.V. Patwardhan, R.D. Kulkarni, Kinetic study of in situ epoxidation of mustard oil, Mol. Catal. 511 (2021), 111748, https://doi.org/10.1016/j.mcat.2021.111748.

[65] E.R. Gunawan, D. Suhendra, P. Arimanda, D. Asnawati, Murniati, Epoxidation of Terminalia catappa L. Seed oil: optimization reaction, South Afr. J. Chem. Eng. 43 (2023) 128–134, https://doi.org/10.1016/j.sajce.2022.10.011.

[66] C.V. Rajput, R.B. Mukherjee, N.V. Sastry, N.P. Chikhaliya, Extraction, characterization and epoxidation of Cassia fistula (Indian laburnum) seed oil: a bio-based material, Ind. Crops Prod. 187 (2022), 115496, https://doi.org/10.1016/j.indcrop.2022.115496.

[67] S.M. Danov, O.A. Kazantsev, A.L. Esipovich, A.S. Belousov, A.E. Rogozhin, E.A. Kanakov, Recent advances in the field of the selective epoxidation of vegetable oils and their derivatives: a review and perspective, Catal. Sci. Technol. 7 (17) (2017) 3659–3675.

[68] G. Wypych, PVC Degradation and Stabilization, Chem Tec Publishing, Toronto, 2015.

[69] J.A. Araujo, Y.J. Cortese, M. Mojicevic, M. Brennan Fournet, Y. Chen, Composite films of thermoplastic starch and CaCl2 extracted from eggshells for extending food shelf-life, Polysaccharides 2 (3) (2021) 677–690, https://doi.org/10.3390/polysaccharides2030041.

[70] A.I. Al-Mosawi, A novel evaluation method for dehydrochlorination of plasticized Poly(vinyl chloride) containing heavy metal-free thermal stabilizing synergistic agent, Polym. Adv. Technol. 32 (8) (2021) 3278–3286, https://doi.org/10.1002/pat.5339.

[71] L. Ma, Y. Lu, Y. Chen, Y. Lu, G. Yuan, Dehydrochlorination study of plasticized poly(vinyl chloride) containing modified titanium dioxide, cerium stearate, organotin and β-diketone complex after long-term storage, Mater. Res. Express 9 (2) (2022), 025305, https://doi.org/10.1088/2053-1591/ac4f87.

[72] W. Han, M. Zhang, D. Li, T. Dong, B. Ai, J. Dou, H. Sun, Design and synthesis of a new mannitol stearate ester-based aluminum alkoxide as a novel tri-functional additive for poly(vinyl chloride) and its synergistic effect with zinc stearate, Polymers 11 (6) (2019) 1031, https://doi.org/10.3390/polym11061031.

[73] W. Han, M. Zhang, Y. Kong, D. Li, L. Liu, S. Tang, J. Ding, S. Liu, Pentaerythritol stearate ester-based tin (II) metal alkoxides: a tri-functional organotin as poly (vinyl chloride) thermal stabilizers, Polym. Degrad. Stabil. 175 (2020), 109129, https://doi.org/10.1016/j.polymdegradstab.2020.109129.

[74] H. Hosney, B. Nadiem, I. Ashour, I. Mustafa, A. El-Shibiny, Epoxidized vegetable oil and bio-based materials as PVC plasticizer, J. Appl. Polym. Sci. 135 (20) (2018), 46270, https://doi.org/10.1002/app.46270.

[75] M. Kurańska, H. Beneš, A. Prociak, O. Trhlíková, Z. Walterová, W. Stochlińska, Investigation of epoxidation of used cooking oils with homogeneous and heterogeneous catalysts, J. Clean. Prod. 236 (2019), 117615, https://doi.org/10.1016/j.jclepro.2019.117615.

[76] R. Ortega-Toro, A. López-Córdoba, F. Avalos-Belmontes, Epoxidized sesame oil as a biobased coupling agent and plasticizer in polylactic acid/thermoplastic yam starch blends, Heliyon 7 (2) (2021), e06176, https://doi.org/10.1016/j.heliyon.2021.e06176.

[77] P.T. Wai, P. Jiang, Y. Shen, P. Zhang, Q. Gu, Y. Leng, Catalytic developments in the epoxidation of vegetable oils and the analysis methods of epoxidized products, RSC Adv. 9 (65) (2019) 38119–38136, https://doi.org/10.1039/c9ra05943a.
[78] P.G. Nihul, S.T. Mhaske, V.V. Shertukde, Epoxidized rice bran oil (ERBO) as a plasticizer for poly(vinyl chloride) (PVC), Iran, Polym. J. 23 (8) (2014) 599–608, https://doi.org/10.1007/s13726-014-0254-7.
[79] D. Braun, H. Cherdron, M. Rehahn, H. Ritter, B. Voit, Polymer Synthesis: Theory and Practice, Springer, Berlin, 2015.
[80] I.N. Vikhareva, G.K. Aminova, A.K. Mazitova, Study of the rheological properties of PVC composites plasticized with butoxyethyl adipates, ChemEngineering 5 (4) (2021) 85, https://doi.org/10.3390/chemengineering5040085.
[81] N. Gupta, P.L. Ramkumar, Experimental investigation of linear low density polyethylene composites based on coir for rotational molding process, Polym. Polym. Compos. 29 (8) (2020) 1114–1125, https://doi.org/10.1177/0967391120953246.
[82] B. Younes, Simple rheological analysis method of spinnable-polymer flow properties using MFI tester, Indian J. Mater. Sci. 2015 (2015) 1–8, https://doi.org/10.1155/2015/790107.
[83] S. Patrick, PVC Compounds and Processing, Smithers Rapra Publishing, Shawbury, United Kingdom, 2004.
[84] N. Teufel, Internal lubricants: process additives yield profits and productivity, Plastics, Addit. Compd. 3 (1) (2001) 26–29, https://doi.org/10.1016/s1464-391x(01)80031-3.
[85] J.W. Summers, Lubrication mechanism of poly(vinyl chloride) compounds: changes upon PVC fusion (gelation), J. Vinyl Addit. Technol. 11 (2) (2005) 57–62, https://doi.org/10.1002/vnl.20037.
[86] S. Al-Malaika, F. Axtell, R. Rothon, M. Gilbert, Chapter 7 - Additives for Plastics in Brydson's Plastics Materials, Butterworth-Heinemann, 2017, https://doi.org/10.1016/B978-0-323-35824-8.00007-4.